XVI International Conference on Computational Plasticity. Fundamentals and Applications
COMPLAS 2021
E. Oñate, D. Peric, M. Chiumenti and Eduardo de Souza Neto (Eds)

THERMOMECHANICAL FEM-BASED MODELLING FOR SEMI-CRYSTALLINE POLYMERS EXHIBITING THE DOUBLE YIELD PHENOMENON

P. HAO[†,*], V. LAHERI[†] AND F.A. GILABERT[†]

[†] Department of Materials, Textiles and Chemical Engineering
Ghent University
Building 46, 9052 Zwijnaarde, Belgium
e-mail: pei.hao@ugent.be, vikram.laheri@ugent.be, fran.gilabert@ugent.be,
web page: https://materialmodels.ugent.be/

[*] SIM M3 program, 9052 Zwijnaarde, Belgium

Key words: Double yield phenomenon, Constitutive model, Semi-crystalline polymer, self-heating, Rate sensitivity

Abstract. Double yield is a common phenomenon observed in a variety of semi-crystalline polymers (SCPs), but the time-dependent double yield points still pose difficulties to be quantitatively captured. Tests conducted at moderate strain rates reveal a characteristic "hump" at the first yield taking place in the amorphous phase. Increasing the applied strain-rate also raises both yield points, although possible thermal softening due to self-heating might cause a dropdown trend under large strains. We introduce a new approach considering the amorphous and crystalline phases to tackle SCPs more practically under the finite strain kinematic framework. To connect the responses of both phases, a procedure based on the yield kinetics is proposed to operate the inelastic deformation gradient of the crystalline phase via the right stretch tensor. A characteristic time is introduced to control the saturated state in the amorphous phase and disclose the "hump". The temperature evolution is updated by solving the energy balance equation via plastic dissipation, which is used to feed the temperature-dependent properties. The simulated results show that the proposed thermomechanical constitutive model is capable to efficiently predict the double yield phenomenon as well as the stress-strain curves at different strain rates with minimum experimental datasets.

1 INTRODUCTION

Double yield phenomenon were documented within a variety of SCPs, for instance, polyamide (PA) [1, 2, 3], polybutyleneterephthalate (PBT) [4], and polyethylene (PE) [5, 6]. A representative stress-strain curve of HDPE is shown in Fig. 1 with double yield points. Two local maximum stresses, σ_{y1} and σ_{y2}, can be found, corresponding to the first and second yield stress. The first yield point is due to the breakthrough of the energy barrier related to the intermolecular resistance in the amorphous domain, whereas the second one can be explained by the slip of the crystalline nanoblocks (crystalline

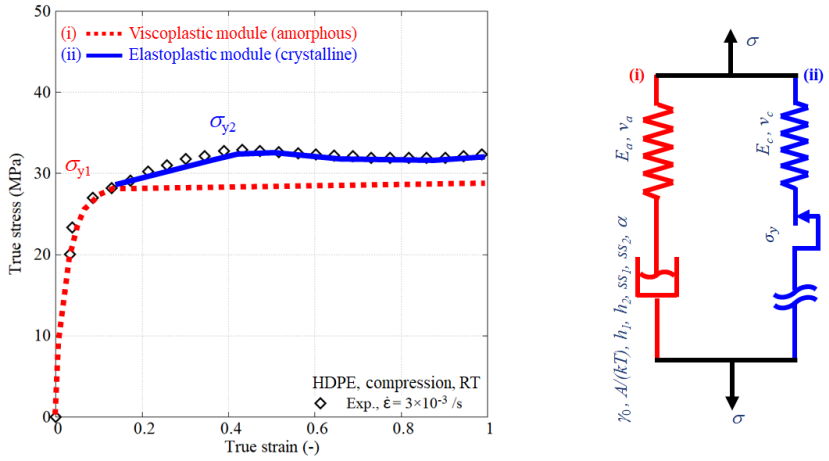

Figure 1: (a) schematic representation of the stress-strain behaviour with amorphous and crystalline contributions. (b) Rheological model.

lamellae) [6, 7], similar to the plastic flow taking place in some metal-based poly-crystalline materials. Few literatures can be found for the experimental investigation of the yield kinetics of SCPs. The plastic deformation in polybutylene (PB) and PA6 has been studied under tensile drawing within micro and nano scales by Atomic Force Microscopy (AFM) [8, 9]. The morphological changes have been observed where the crystal lamellae align to the draw direction and shear bands are formed.

Several constitutive models have been developed targeting SCPs within different approaches like the micromechanics framework [6, 7], homogenization process with explicit representation of the crystallization degree [10] and homogeneous models considering an effective amorphous-crystalline phase [11]. However, in all of them the double yield phenomenon has only be captured qualitatively. Besides, some of these models require multiple fitting parameters, reducing its applicability in realistic engineering contexts. Thus, the aim of this work is to propose a new approach to facilitate the understanding and the material characterization of SCPs.

In the following, the proposed double yield model is introduced with two modules accounting for the amorphous and crystalline domains. Finite strain kinematics framework is elaborated according to the rheological model arrangement. The experimental results of HDPE and nylon 101 available in the literature are chosen to calibrate and validate the proposed model.

2 KINEMATICS

The finite strain kinematics framework allow us to incorporate the new constitutive model in rate form in an intuitive manner. The total deformation gradient is assigned to each phase (amorphous and crystalline) assuming a connection in parallel (see Fig. 1b) as

$$\boldsymbol{F}^{\mathrm{a}} = \boldsymbol{F}^{\mathrm{c}} = \boldsymbol{F}, \tag{1}$$

where $\boldsymbol{F}^{\mathrm{a}}$ and $\boldsymbol{F}^{\mathrm{c}}$ are the deformation gradients applied on the amorphous and crystalline branches (i) and (ii).

The amorphous one $\boldsymbol{F}^{\mathrm{a}}$ can be decomposed multiplicatively into two components to describe the inelastic response. The elastic part $\boldsymbol{F}^{\mathrm{a}}_{\mathrm{e}}$ is calculated by removing the inelastic part $\boldsymbol{F}^{\mathrm{a}}_{\mathrm{p}}$ as follow

$$\boldsymbol{F}^{\mathrm{a}}_{\mathrm{e}} = \boldsymbol{F}^{\mathrm{a}} \cdot \boldsymbol{F}^{\mathrm{a}-1}_{\mathrm{p}}, \tag{2}$$

where the rate of deformation gradient change can be expressed as $\dot{\boldsymbol{F}}^{\mathrm{a}}_{\mathrm{p}} = \boldsymbol{D}^{\mathrm{a}}_{\mathrm{p}}\boldsymbol{F}^{\mathrm{a}}_{\mathrm{p}}$ with a spin-free plastic velocity gradient $\boldsymbol{W}^{\mathrm{a}}_{\mathrm{p}} = 0$ for an isotropic material [12]. The inelastic rate of deformation $\boldsymbol{D}^{\mathrm{a}}_{\mathrm{p}}$ is further presented in the next section.

The Cauchy elastic stress tensor contributed from the amorphous phase is given by

$$\boldsymbol{\sigma}^{\mathrm{a}} = \frac{1}{\det\left[\boldsymbol{F}^{\mathrm{a}}_{\mathrm{e}}\right]}(\lambda \operatorname{tr}[\boldsymbol{h}]\boldsymbol{I} + 2\mu\boldsymbol{h}), \tag{3}$$

where λ and μ are the Lame parameters, $\boldsymbol{h} = \log\left(\sqrt{\boldsymbol{B}_{\mathrm{e}}}\right)$ is the Hencky strain tensor with the elastic Cauchy-Green tensor $\boldsymbol{B}$, and $\boldsymbol{I}$ is the identity tensor.

It is noticed that the contribution of the crystalline domain is only activated as long as the first yield point is reached. In other words, once the saturated state of the amorphous domain is reached, the crystalline phase will be switched on. This is in accordance with the experimental observation in morphological changes [9]. To do this, the deformation gradient on the crystalline phase has to be delayed according to the amorphous one. Here, the right stretch tensor $\boldsymbol{U} = \boldsymbol{R}^{-1}\boldsymbol{F}$ is calculated on the fly and stored as an internal variable. The offset right stretch tensor $\boldsymbol{U}_{\mathrm{off}}$ is determined at the moment that the plastic flow rate becomes equal to the applied strain rate (yield definition of amorphous polymer). The deformation gradient on the crystalline phase is then updated as follows

$$\boldsymbol{F}^{\mathrm{c}} = \boldsymbol{R}\left(\boldsymbol{R}^{-1}\boldsymbol{F} - \boldsymbol{U}_{\mathrm{off}}\right) + \boldsymbol{I}. \tag{4}$$

Finally, the total Cauchy elastic stress tensor can be expressed in terms of amorphous and crystalline components, given by

$$\boldsymbol{\sigma}^{\mathrm{total}} = \boldsymbol{\sigma}^{\mathrm{a}} + \boldsymbol{\sigma}^{\mathrm{c}}, \tag{5}$$

3 CONSTITUTIVE MODEL

To cover the prescribed double yield phenomenon as well as the rate- and temperature-dependencies, two independent components were chosen to construct the rheological model (Fig. 1). The corresponding stress-strain behaviour of amorphous and crystalline components is depicted along with the experimental curve of HDPE.

Either phenomenological or physical model may be chosen under the proposed framework. The chosen models should follow the main principles as developed for glassy amorphous polymer and for poly crystalline materials. The main objective of this work is to show how to use appropriately the model combination to capture the double yielding points by considering the modification of kinematic framework.

3.1 Amorphous

The macromolecular Boyce-Parks-Argon (BPA) model based on the double kink theory for glassy amorphous polymers was used [12]. This theory has been successfully applied to describe a wide variety of thermoplastic polymers as PMMA, PC or PS [13, 14, 15]. Further modification has been made by Chowdhury et al [16]. By introducing a heaviside-like function for the pre-yield nonlinearity, this rate- and temperature- dependent viscoplastic model was also validated with experimental results of Epoxy [17]. The inelastic rate of deformation $\boldsymbol{D}_{\mathrm{p}}^{\mathrm{a}} = \dot{\bar{\epsilon}}\boldsymbol{N}$ is related to the following prescribed constitutive law expressed as

$$\dot{\bar{\epsilon}} = \dot{\epsilon}_0 \exp\left[-\frac{A\left(s-\alpha\sigma_{\mathrm{h}}\right)}{K_B\theta}\left(1-\left(\frac{\sigma_{\mathrm{e}}}{s-\alpha\sigma_{\mathrm{h}}}\right)^m\right)\right], \tag{6}$$

where $\dot{\epsilon}_0$, m and A are rate sensitivity parameters, controlling the first yield stress at different strain rates, s is the athermal stress that is related to the micro structure of the polymer chain, σ_{e} and σ_{h} are the equivalent driving stress and the trace of Cauchy stress of amorphous contribution, α is the pressure sensitivity parameter, θ is the absolute temperature and K_B is the Boltzmann constant (details refer to Ref. [17]).

3.2 Crystalline

Pressure-dependent elastoplasticity using the paraboloidal yield criterion was adopted in this case. This criterion is a function of the equivalent stress $\bar{\sigma}$ of crystalline contribution and the corresponding yield stresses in compression σ_{yc} and tension σ_{yt} given by

$$\phi(\boldsymbol{\sigma}) = \bar{\sigma}^2 - \left(\sigma_{\mathrm{yt}} - \sigma_{\mathrm{yc}}\right) I_1 - \sigma_{\mathrm{yt}}\sigma_{\mathrm{yc}}, \tag{7}$$

where I_1 is the first invariant of stress tensor, $I_1 = \boldsymbol{\sigma} : \mathbf{I} = -3p$.

This material model was implemented by using a non-iterative algorithmic scheme for associated and non-associated flow rules [18]. This novel scheme highly improves the computational efficiency compared to the conventional implementation of traditional radial return mapping algorithms. The plastic multiplier is the absolute solution of the quadratic equation which fulfils the Kuhn-Tucker's loading-unloading consistency conditions. For associated flow rule the quadratic equation as a function of plastic strain increment is derived as

$$\left[4\left(\bar{\sigma}^{tr}\right)^2\left(9\mu^2 - h^2\right)\right]\Delta\gamma^2 - \left[12\mu\left(\bar{\sigma}^{tr}\right)^2 + 2h\left(\sigma_{\mathrm{yt}} + \sigma_{\mathrm{yc}}\right)\bar{\sigma}^{tr} + 9\kappa\left(\sigma_{\mathrm{yt}} - \sigma_{\mathrm{yc}}\right)^2\right]\Delta\gamma + \phi^{tr} = 0. \tag{8}$$

According to the experimental observation, a non-linear hardening table is provided to demonstrate the study cases of HDPE [6] and nylon 101 [1], respectively. Both experiments were conducted under compression.

4 THERMOMECHANICAL COUPLING

Thermomechanical coupling analyses are essential because the engineering applications using SCPs are greatly affected by the temperature and the mechanical properties

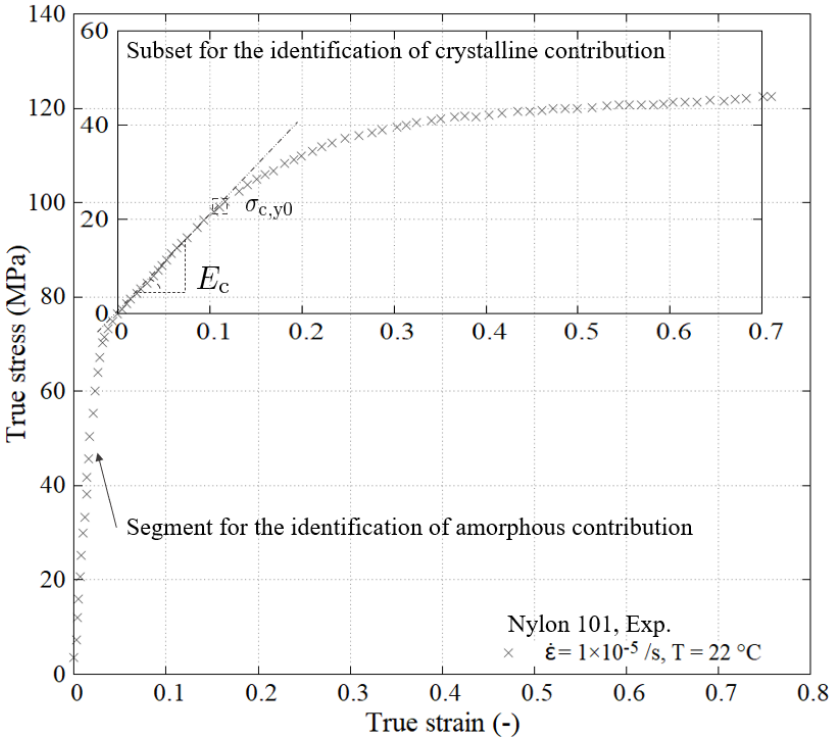

Figure 2: Representative isothermal stress-strain curve at the lowest strain rate in room temperature.

degrade due to the self-heating. Garcia-Gonzalez *et al.* [19] proposed a hyperelastic-thermoviscoplastic constitutive model for semi-crystalline polymers and successfully applied to PEEK. It was concluded that the thermal softening occurs in the intermolecular resistance (amorphous domain in our proposed model).

The proposed rate-dependent model covers a wide range of strain rates, nevertheless, the self-heating and thermal softening effects are more pronounced at high strain rates. Three regimes can be classified: isothermal, fully coupled and nearly adiabatic. By comparing the testing period ($t_{test} = 1.0/\dot{\epsilon}$) to the estimated thermal diffusion time ($t_d = \frac{L^2}{2(k/\rho c)}$) the corresponding regime can be easily determined (see Ref. [14]). The thermomechanical coupling is realized by calculating the inelastic fraction η of the rate of plastic dissipation energy and feeding the rate of heat generation $\dot{q}$ to solve the general energy balance equation given by

$$\rho c\dot{\theta} - \operatorname{div}(k \operatorname{grad} \theta) = \dot{q}. \tag{9}$$

The thermal softening can be captured by updating the resolved temperature field for the amorphous model.

5 MATERIAL CHARACTERIZATION

The material calibration is an essential stage to ensure the model functionality. The parameter identification (PI) procedure is briefly introduced. For the non-isothermal cases HDPE and nylon 101 presented below, five tests are required:

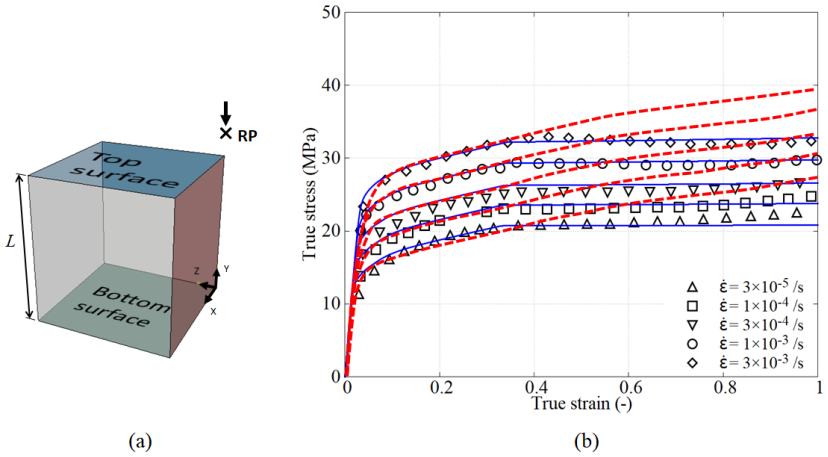

(a) (b)

Figure 3: (a) SE model assuming isothermal condition. (b) True compressive stress-strain curves compared to experimental results (symbols): prediction by micromechanical model(dash lines) and double yield model (solid lines) at different strain rates and room temperature (RT).

1. Three cylinder compression tests at different strain rates ($\dot{\epsilon}_1 < \dot{\epsilon}_2 < \dot{\epsilon}_3$) and a chosen reference temperature, $T_{\text{ref}} < T_{\text{g}}$ (glass transition temperature).

2. Two tests at two different temperatures between T_{ref} and T_{g} and same strain rates as $\dot{\epsilon}_1$.

According to the proposed kinematics, Fig. 2 shows two separated segments for the identification of amorphous and crystalline phases individually. The amorphous one is used to calibrate the first yield part, and the PI process is given by Ref. [17]. The elastoplastic response of crystalline is determined within the sub-window with an offset origin to the initial point of linear elastic phase after the first yield point is reached. More details on the underlying yield kinetics and PI process will be published in a forthcoming paper [20].

6 RESULTS

6.1 HDPE - isothermal analysis

The single element (SE) simulation with isothermal condition presented was employed using an implicit solver. The applied temperature is directly fixed in the user material subroutine with a value of 25 °C so that the temperature coupling is deactivated for a maximum strain rate $3 \times 10^{-3}/s$. The SE model consists of a hexahedral element with side length $L = 1$ mm (Fig. 3a). The stress and strain components along the compressive direction at the integration point were extracted for analysis.

Fig. 3b shows the true stress-true strain comparison between the experimental results and two types of predictions. Both the micromechanics model and our proposed double yield model can capture the double yield phenomenon. The first yield point is captured well by both models at a strain around 5%. However, the second yield point visible in the true stress-true strain curves can only be quantitatively predicted by the proposed model

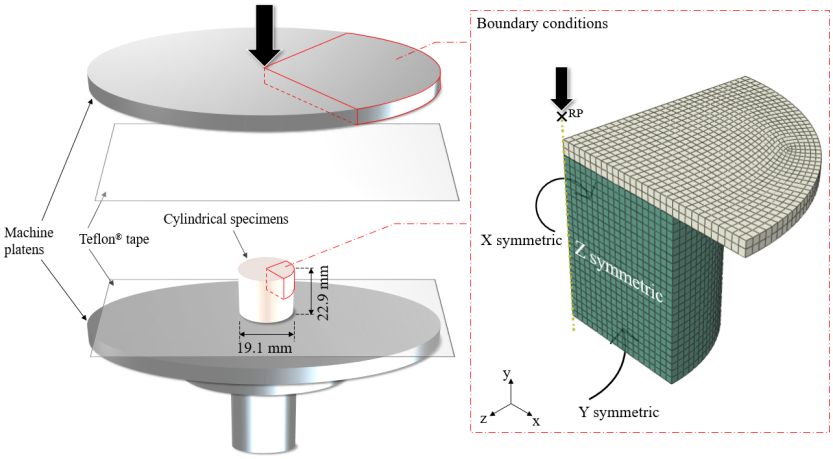

Figure 4: FEM of cylinder compression set-up for nylon 101.

at a strain around 37%. Within these strain rates, it can be noticed that the experimental curves are distributed evenly in parallel, which confirms that the crystalline contribution is rate independent for this HDPE. The rate dependency is controlled by the amorphous domain with clear distribution of the first yield point spreading from 14 to 27 MPa when the strain rate is increased from $3 \times 10^{-5}/s$ to $3 \times 10^{-3}/s$.

6.2 Nylon 101 - thermomechanical coupled analysis

Thermal softening effect is observed from the experiments where a maximum strain rate $1/s$ was applied [1]. Thermomechanical analysis was performed and a one-eighth realistic compressive cylinder specimen with symmetric boundary conditions on the inner surfaces was modelled along with metal compressive platen. Fig. 4 shows the set-up and the corresponding FEM with its dimensions. The thermal properties are listed in Table 1. The contact surfaces were assumed frictionless to mimic the applied Teflon tapes. The contact conductance was chosen the same as the metal one. Natural convection was assumed and applied as boundary condition to the outer curved surface to a sink temperature of 22 °C with a convection coefficient $h = 10$ W/(m^2 C). The volume-averaged homogenization was used to obtain the true stress-true strain curves.

Table 1: Thermal properties of nylon 101 and metal platens.

	ρ (kg/m^3)	c (J/kg K)	k (J/s m K)
Nylon 101	1200	1700	0.25
Steel	7800	420	52

Fig. 5 plots the homogenized stress-strain curves, and double yield points were accurately predicted. "Small humps" at strain rates $1 \times 10^{-2}/s$ and $1/s$ are also captured by the proposed model with introducing a characteristic time which accounts for the equilib-

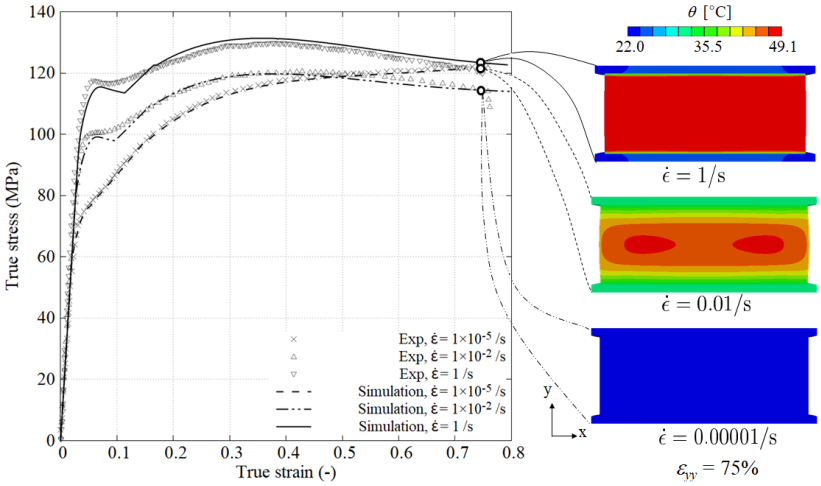

Figure 5: True stress-strain curves and internal temperature field of nylon 101 at strain rates $1 \times 10^{-5}/s$, $1 \times 10^{-2}/s$ and $1/s$.

rium state established among amorphous and crystalline regions. The realistic cylinder model was simulated in nearly adiabatic condition and compared with the experimental stress-strain curve at strain rate of $1/s$, resulting in an inelastic fraction, $\eta = 1.0$.

Fig. 5 also shows the temperature profile at strain of 75% for three strain rates. The comparison is drawn with the same legend gauge for all three conditions with different strain rates from the initial temperature 22 °C to the maximum 49.1 °C obtained from the adiabatic condition. The experimental testing time for the isothermal condition with the strain rate $1 \times 10^{-5}/s$ is around 21 hours assuming a constant strain rate. This long period allows for an efficient thermal diffusion and the temperature changes in the specimen was barely observed. On the contrary, the short testing time of 0.75 s at the fastest strain rate $1/s$ is insufficient to decrease the temperature rise caused by the self-heating from the specimen. The heat cannot even be conducted to the metal platens as shown Fig. 5, whereas in the coupled condition, the temperature in metal platens is obviously increased above 30 °C.

7 CONCLUSIONS

This work proposes a constitutive material model capable to capture the double yield phenomenon observed in a wide variety of semi-crystalline polymers. The idea relies on combining two rheological analogue branches connected in parallel. One branch provides a full thermo-mechanical rate-dependent response for the amorphous phase, whilst the other introduces the rate-independent response of the crystalline domains.

Unlike other approaches, the present proposal demands a low number of experimental results, making it very suitable for the design and further development of advanced thermoplastics. The model proves an excellent agreement with HDPE and Nylon 101, although it can be easily extended to other thermoplastics. Further research on its mechanical response above the glass transition temperature is currently ongoing, as well as a more extensive validation process.

ACKNOWLEDGEMENTS

The work leading to this abstract has been funded by the ICON project "ProPeL", which fits in the MacroModelMat (M3) research program, coordinated by Siemens (Siemens Digital Industries Software, Belgium), and funded by SIM (Strategic Initiative Materials in Flanders) and VLAIO (Flemish government agency Flanders Innovation & Entrepreneurship). Financial support from "Bijzonder Onderzoeksfonds" (BOF.STG.2018.0030.01) by Ghent University is also gratefully acknowledged.

REFERENCES

[1] Khan, A.S. and Farrokh, B. Thermo-mechanical response of nylon 101 under uniaxial and multi-axial loadings: Part I, Experimental results over wide ranges of temperatures and strain rates. *Int. J. Plast.* (2006) **22**:1506-1529.

[2] Laiarinandrasana, L., Selles, N., Klinkova, O., Morgeneyer, T.F., Proudhon, H., and Helfen, L. Structural versus microstructural evolution of semi-crystalline polymers during necking under tension: Influence of the skin-core effects, the relative humidity and the strain rate. *Polym. Test.* (2016) **55**:297-309.

[3] Parodi, E., Peters, G.W.M., and Govaert, L.E. Prediction of plasticity-controlled failure in polyamide 6: Influence of temperature and relative humidity. *J. Appl. Polym. Sci.* (2018) **135**(11):45942.

[4] Zhang, J. Study of poly(trimethylene terephthalate) as an engineering thermoplastics material. *J. Appl. Polym. Sci.* (2004) **91**(3):1657-1666.

[5] Brooks, N.W., Duckett, R.A., and Ward, I.M. Investigation into double yield points in polyethylene. *Polymers* (1992) **33**(9):1872-1880.

[6] Sedighiamiri, A., Govaert, L.E., and van Dommelen, J.A.W. Micromechanical modeling of the deformation kinetics of semicrystalline polymers. *J. Polym. Sci. Pol. Phys.* (2011) **49**(18):1297-1310.

[7] Uchida, M. and Tada, N. Micro-, meso- to macroscopic modeling of deformation behavior of semi-crystalline polymer. *Int. J. Plast.* (2013) **49**:164-184.

[8] Ferreiro, V. and Coulon, G. Shear banding in strained semicrystalline polyamide 6 films as revealed by atomic force microscopy: Role of the amorphous phase. *J. Polym. Sci. Pol. Phys.* (2004) **42**(4):687-701.

[9] Thomas, C., Seguela, R., Detrez, F., Miri, V., and Vanmansart, C. Plastic deformation of spherulitic semi-crystalline polymers: An in situ AFM study of polybutene under tensile drawing. *Polymers* (2009) **50**(15):3714-3723.

[10] Ayoub, G., Zaïri, F., Naït-Abdelaziz, M., and Gloaguen, J.M. Effects of crystal content on the mechanical behaviour of polyethylene under finite strains: Experiments and constitutive modelling. *Int. J. Plast.* (2011) **27**:492-511.

[11] Maurel-Pantel, A., Baquet, E., Bikard, J., Bouvard, J.L., and Billon, N. A thermo-mechanical large deformation constitutive model for polymers based on material network description: Application to a semi-crystalline polyamide 66. *Int. J. Plast.* (2014) **67**:102-126.

[12] Boyce, M.C., Parks, D.M., and Argon, A.S. Large inelastic deformation of glassy polymers. part I: rate dependent constitutive model. *Mech. Mater.* (1988) **7**(1):15-33.

[13] Boyce, M.C., Arruda, E.M., and Jayachandran, R. The large strain compression, tension, and simple shear of polycarbonate. *Polym. Eng. Sci.* (1994) **34**(9):716-725.

[14] Arruda, E.M., Boyce, M.C., and Jayachandran, R. Effects of strain rate, temperature and thermomechanical coupling on the finite strain deformation of glassy polymers. *Mech. Mater.* (1995) **19**(2-3):193-212.

[15] Mulliken, A.D. and Boyce, M.C. Mechanics of the rate-dependent elasticplastic deformation of glassy polymers from low to high strain rates. *Int. J. Solids. Struct.* (2006) **43**(5):1331-1356.

[16] Chowdhury, K.A., Benzerga, A.A., and Talreja, R. A computational framework for analyzing the dynamic response of glassy polymers. *Comput. Methods Appl. Mech. Engrg.* (2008) **197**:4485-4502.

[17] Poulain, X., Benzerga, A.A., and Goldberg, R.K. Finite-strain elasto-viscoplastic behavior of an epoxy resin: Experiments and modeling in the glassy regime. *Int. J. Plast.* (2014) **62**:138-161.

[18] Laheri, V., Hao, P., and Gilabert, F.A. Efficient and non-iterative algorithmic scheme to model pressure-dependent polymer elastoplasticity using paraboloidal yield criterion. (2021) Manuscript in preparation.

[19] Garcia-Gonzalez, D., Zaera, R., and Arias, A. A hyperelastic-thermoviscoplastic constitutive model for semi-crystalline polymers: Application to PEEK under dynamic loading conditions. *Int. J. Plast.* (2017) **88**:27-52.

[20] Hao, P., Laheri, V., and Gilabert, F.A. Thermo-viscoelastic-viscoplastic double yield model for semi-crystalline thermoplastics below glass transition temperature. (2021) Manuscript in preparation.